Observation of the $\Upsilon(3S)$ meson and suppression of Υ states in PbPb collisions at $\sqrt{s_{\mathrm{NN}}} = 5.02\,\mathrm{TeV}$

—Supplemental Material—

The CMS Collaboration
CERN
(Dated: May 16, 2024)

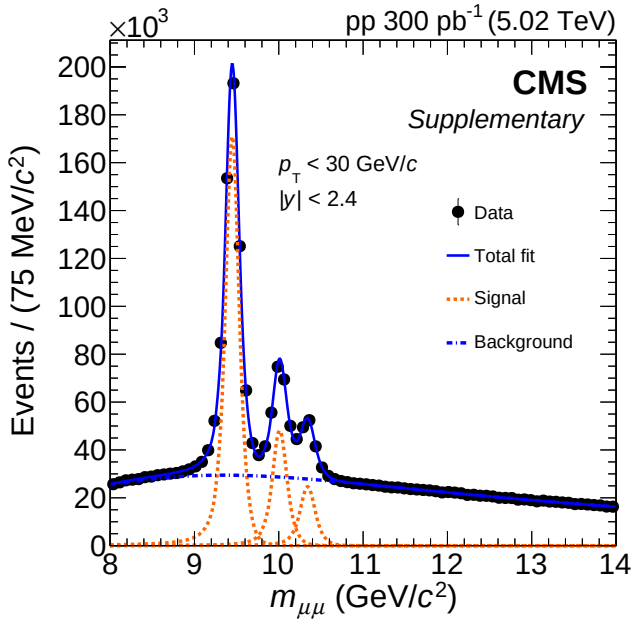

FIG. 1. Dimuon invariant mass distribution in pp collisions, integrated over the full kinematic range $p_{\mathrm{T}} < 30\,\mathrm{GeV}/c$ and $|y| < 2.4$. The solid curves show the result of the fit, whereas the orange dashed and blue dash-dotted curves represent the three Υ states and the background, respectively.

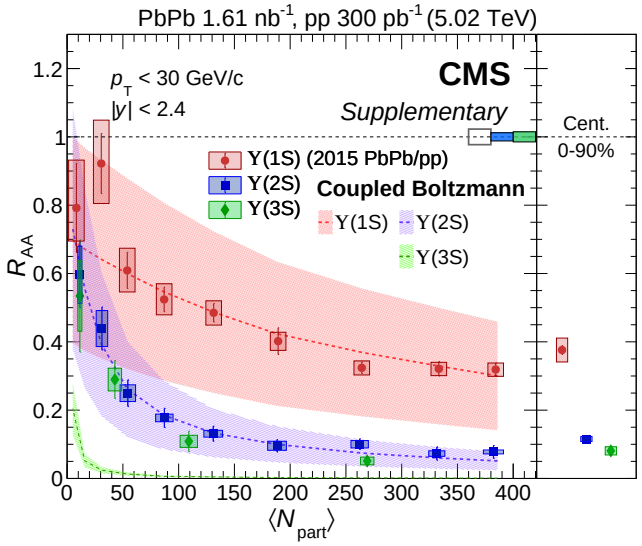

FIG. 2. Nuclear modification factors for the $\Upsilon(1S)$, $\Upsilon(2S)$, and $\Upsilon(3S)$ mesons as a function of $\langle N_{\mathrm{part}}\rangle$(from Figure 2 left), including the centrality integrated bin. The vertical lines and boxes correspond to statistical and systematic uncertainties, respectively. The left-most box at unity combines the uncertainties of pp luminosity and PbPb N_{MB}, while the second (third) box corresponds to the uncertainty of pp yields for the $\Upsilon(2S)$ ($\Upsilon(3S)$) state. Results for the $\Upsilon(1S)$ meson are taken from Ref. [1]. The bands represent calculations from Ref. [2].

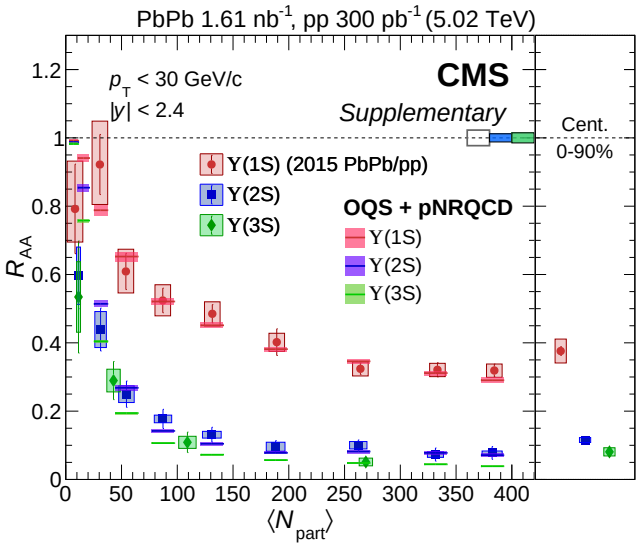

FIG. 3. Nuclear modification factors for the $\Upsilon(1S)$, $\Upsilon(2S)$, and $\Upsilon(3S)$ mesons as a function of $\langle N_{\rm part}\rangle$(from Figure 2 left), including the centrality integrated bin. The vertical lines and boxes correspond to statistical and systematic uncertainties, respectively. The left-most box at unity combines the uncertainties of pp luminosity and PbPb $N_{\rm MB}$, while the second (third) box corresponds to the uncertainty of pp yields for the $\Upsilon(2S)$ ($\Upsilon(3S)$) state. Results for the $\Upsilon(1S)$ meson are taken from Ref. [1]. The OQS + pNRQCD theory calculations are taken from Ref. [3].

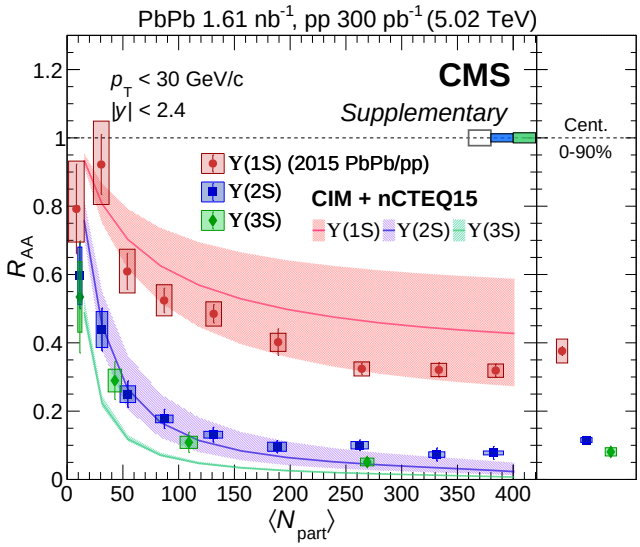

FIG. 4. Nuclear modification factors for the $\Upsilon(1S)$, $\Upsilon(2S)$, and $\Upsilon(3S)$ mesons as a function of $\langle N_{\rm part}\rangle$(from Figure 2 left), including the centrality integrated bin. The vertical lines and boxes correspond to statistical and systematic uncertainties, respectively. The left-most box at unity combines the uncertainties of pp luminosity and PbPb $N_{\rm MB}$, while the second (third) box corresponds to the uncertainty of pp yields for the $\Upsilon(2S)$ ($\Upsilon(3S)$) state. Results for the $\Upsilon(1S)$ meson are taken from Ref. [1]. The bands represent calculations from Ref. [4].

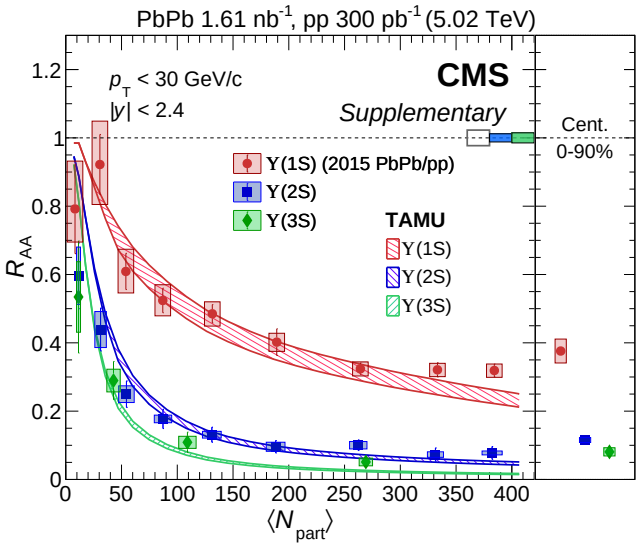

FIG. 5. Nuclear modification factors for the $\Upsilon(1S)$, $\Upsilon(2S)$, and $\Upsilon(3S)$ mesons as a function of $\langle N_{\rm part}\rangle$(from Figure 2 left), including the centrality integrated bin. The vertical lines and boxes correspond to statistical and systematic uncertainties, respectively. The left-most box at unity combines the uncertainties of pp luminosity and PbPb $N_{\rm MB}$, while the second (third) box corresponds to the uncertainty of pp yields for the $\Upsilon(2S)$ ($\Upsilon(3S)$) state. Results for the $\Upsilon(1S)$ meson are taken from Ref. [1]. The bands represent calculations from Ref. [5].

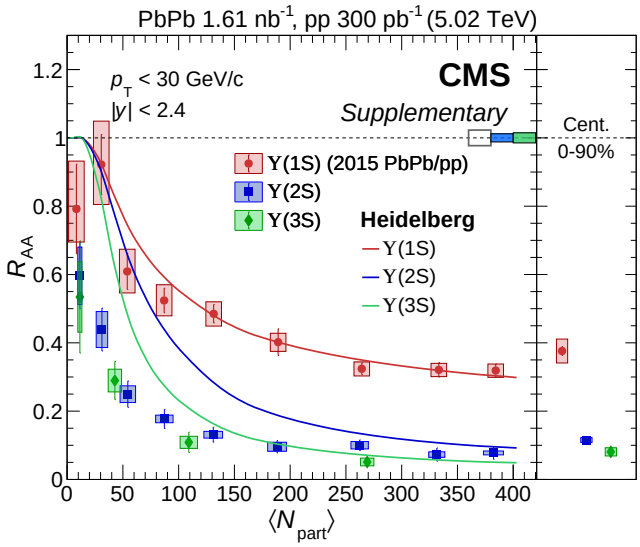

FIG. 6. Nuclear modification factors for the $\Upsilon(1S)$, $\Upsilon(2S)$, and $\Upsilon(3S)$ mesons as a function of $\langle N_{\rm part}\rangle$(from Figure 2 left), including the centrality integrated bin. The vertical lines and boxes correspond to statistical and systematic uncertainties, respectively. The left-most box at unity combines the uncertainties of pp luminosity and PbPb $N_{\rm MB}$, while the second (third) box corresponds to the uncertainty of pp yields for the $\Upsilon(2S)$ ($\Upsilon(3S)$) state. Results for the $\Upsilon(1S)$ meson are taken from Ref. [1]. The lines represent calculations from Ref. [6].

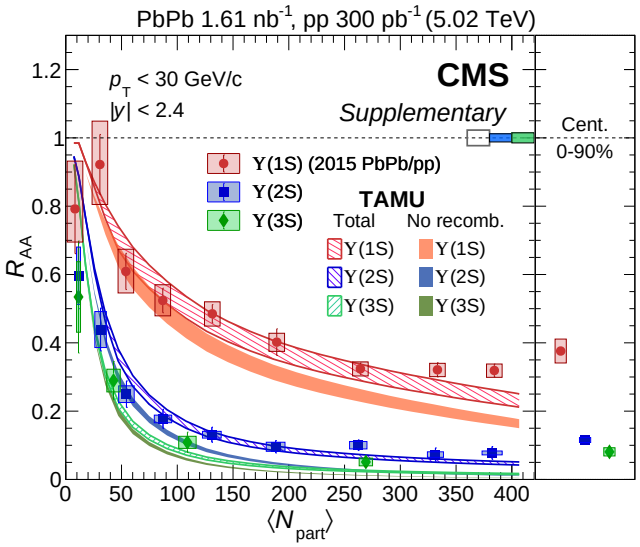

FIG. 7. Nuclear modification factors for the $\Upsilon(1S)$, $\Upsilon(2S)$, and $\Upsilon(3S)$ mesons as a function of $\langle N_{\rm part}\rangle$(from Figure 2 left), including the centrality integrated bin. The vertical lines and boxes correspond to statistical and systematic uncertainties, respectively. The left-most box at unity combines the uncertainties of pp luminosity and PbPb $N_{\rm MB}$, while the second (third) box corresponds to the uncertainty of pp yields for the $\Upsilon(2S)$ ($\Upsilon(3S)$) state. Results for the $\Upsilon(1S)$ meson are taken from Ref. [1]. The two type of bands represent calculations from Ref. [5], with the solid filled bands calculated without the recombination component.

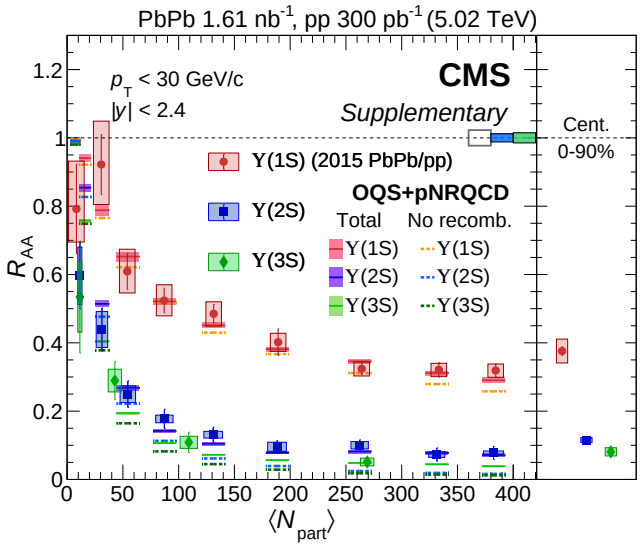

FIG. 8. Nuclear modification factors for the $\Upsilon(1S)$, $\Upsilon(2S)$, and $\Upsilon(3S)$ mesons as a function of $\langle N_{\rm part}\rangle$(from Figure 2 left), including the centrality integrated bin. The vertical lines and boxes correspond to statistical and systematic uncertainties, respectively. The left-most box at unity combines the uncertainties of pp luminosity and PbPb $N_{\rm MB}$, while the second (third) box corresponds to the uncertainty of pp yields for the $\Upsilon(2S)$ ($\Upsilon(3S)$) state. Results for the $\Upsilon(1S)$ meson are taken from Ref. [1]. The OQS + pNRQCD theory calculations are taken from Ref. [3], with the dashed one calculated without the recombination component.

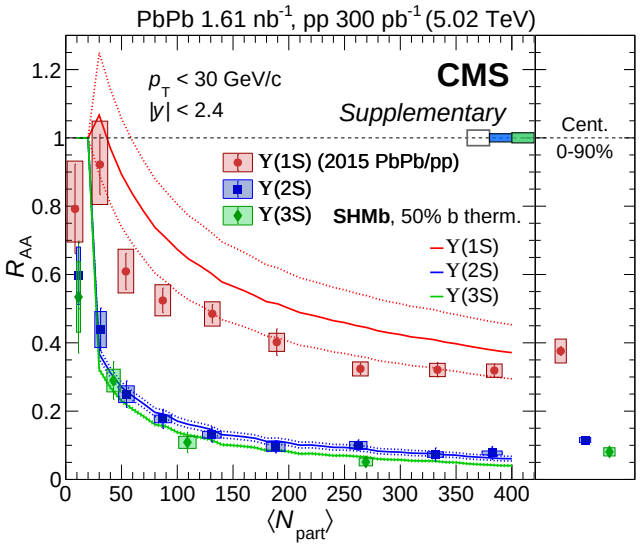

FIG. 9. Nuclear modification factors for the $\Upsilon(1S)$, $\Upsilon(2S)$, and $\Upsilon(3S)$ mesons as a function of $\langle N_{\mathrm{part}}\rangle$(from Figure 2 left), including the centrality integrated bin. The vertical lines and boxes correspond to statistical and systematic uncertainties, respectively. The left-most box at unity combines the uncertainties of pp luminosity and PbPb N_{MB}, while the second (third) box corresponds to the uncertainty of pp yields for the $\Upsilon(2S)$ ($\Upsilon(3S)$) state. Results for the $\Upsilon(1S)$ meson are taken from Ref. [1]. The lines represent calculations from Ref. [7], with the solid line corresponding to 50% thermalization of the $b\bar{b}$ pairs and the upper and lower dashed lines representing the 20% uncertainty of the total $b\bar{b}$ cross section.

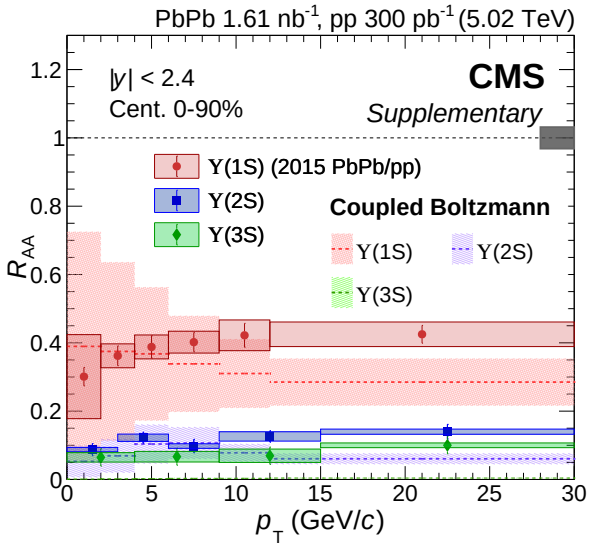

FIG. 10. Nuclear modification factors for the $\Upsilon(1S)$, $\Upsilon(2S)$, and $\Upsilon(3S)$ mesons as a function of p_{T} (from Figure 2 right). The vertical lines and boxes correspond to statistical and systematic uncertainties, respectively. The box at unity represents the global uncertainty, which combines uncertainties from T_{AA}, pp luminosity, and PbPb N_{MB}. Results for the $\Upsilon(1S)$ meson are taken from Ref. [1]. The bands represent calculations from Ref. [2].

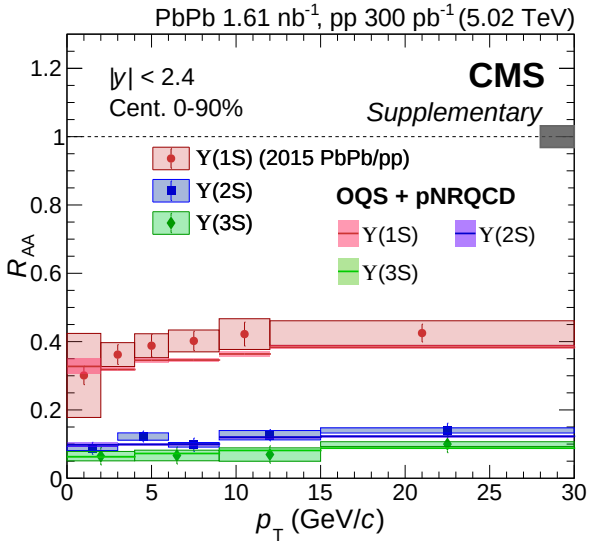

FIG. 11. Nuclear modification factors for the $\Upsilon(1S)$, $\Upsilon(2S)$, and $\Upsilon(3S)$ mesons as a function of p_{T} (from Figure 2 right). The vertical lines and boxes correspond to statistical and systematic uncertainties, respectively. The box at unity represents the global uncertainty, which combines uncertainties from T_{AA}, pp luminosity, and PbPb N_{MB}. Results for the $\Upsilon(1S)$ meson are taken from Ref. [1]. The OQS + pNRQCD theory calculations are taken from Ref. [3].

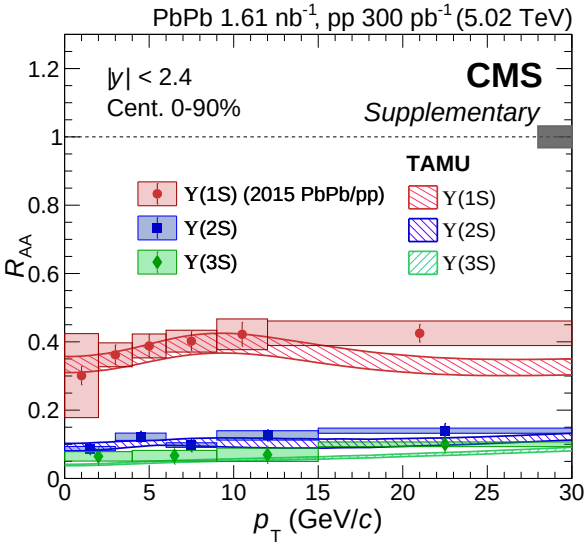

FIG. 12. Nuclear modification factors for the $\Upsilon(1S)$, $\Upsilon(2S)$, and $\Upsilon(3S)$ mesons as a function of p_{T} (from Figure 2 right). The vertical lines and boxes correspond to statistical and systematic uncertainties, respectively. The box at unity represents the global uncertainty, which combines uncertainties from T_{AA}, pp luminosity, and PbPb N_{MB}. Results for the $\Upsilon(1S)$ meson are taken from Ref. [1]. The bands represent calculations from Ref. [5].

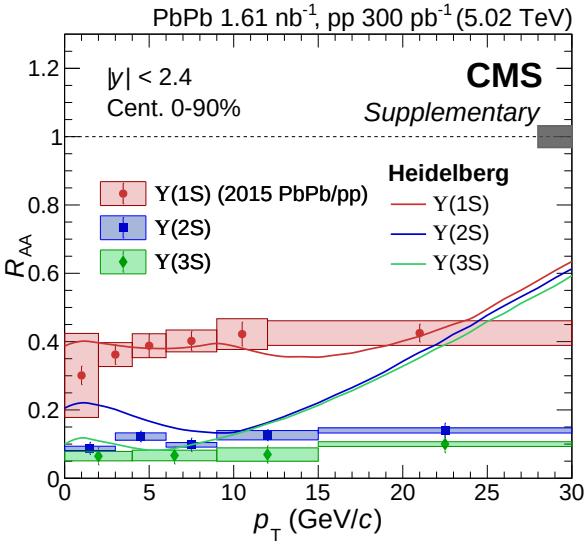

FIG. 13. Nuclear modification factors for the $\Upsilon(1S)$, $\Upsilon(2S)$, and $\Upsilon(3S)$ mesons as a function of p_{T} (from 2 right). The vertical lines and boxes correspond to statistical and systematic uncertainties, respectively. The box at unity represents the global uncertainty, which combines uncertainties from T_{AA}, pp luminosity, and PbPb N_{MB}. Results for the $\Upsilon(1S)$ meson are taken from Ref. [1]. The lines represent calculations from Ref. [6].

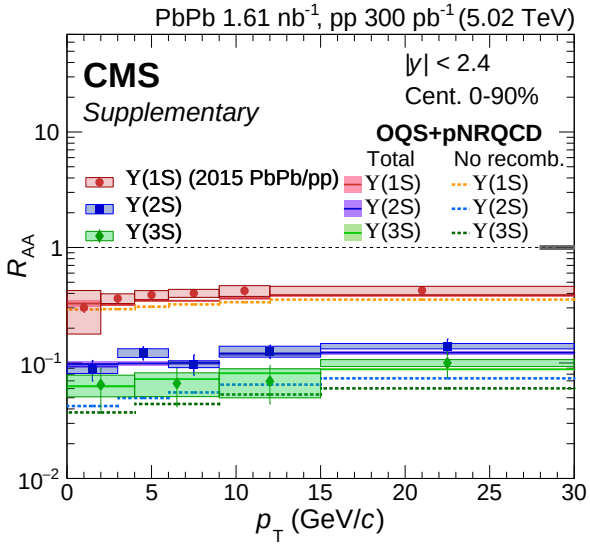

FIG. 14. Nuclear modification factors for the $\Upsilon(1S)$, $\Upsilon(2S)$, and $\Upsilon(3S)$ mesons as a function of p_{T} (from Figure 2 right). The vertical lines and boxes correspond to statistical and systematic uncertainties, respectively. The box at unity represents the global uncertainty, which combines uncertainties from T_{AA}, pp luminosity, and PbPb N_{MB}. Results for the $\Upsilon(1S)$ meson are taken from Ref. [1]. The OQS + pNRQCD theory calculations are taken from Ref. [3], with the dashed one calculated without the recombination component.

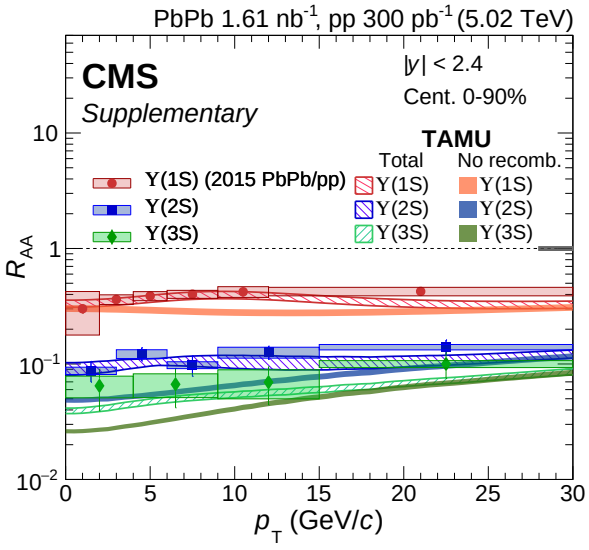

FIG. 15. Nuclear modification factors for the $\Upsilon(1S)$, $\Upsilon(2S)$, and $\Upsilon(3S)$ mesons as a function of p_{T} (from Figure 2 right). The vertical lines and boxes correspond to statistical and systematic uncertainties, respectively. The box at unity represents the global uncertainty, which combines uncertainties from T_{AA}, pp luminosity, and PbPb N_{MB}. Results for the $\Upsilon(1S)$ meson are taken from Ref. [1]. The two type of bands represent calculations from Ref. [5], with the solid filled bands calculated without the recombination component.

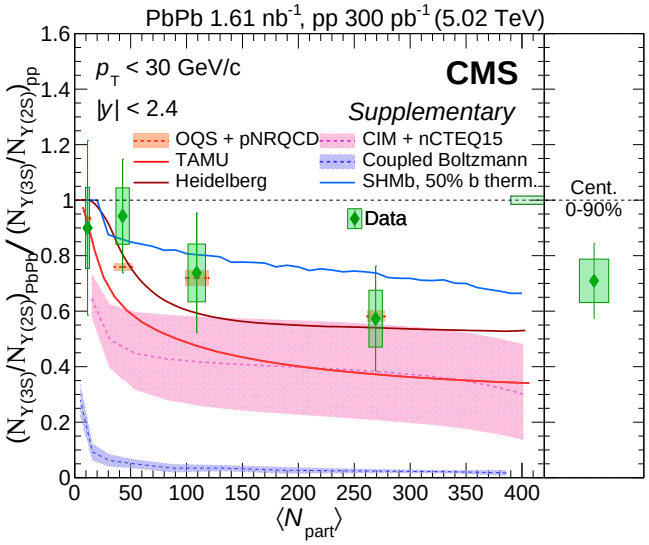

FIG. 16. The double ratio of $\Upsilon(3S)/\Upsilon(2S)$ as functions of $\langle N_{\mathrm{part}}\rangle$(from Figure 3 left). The vertical lines correspond to statistical uncertainties, while the boxes are the systematic uncertainties. The box at unity shows the combined systematic and statistical uncertainties from pp data. The six different types of lines and bands represent calculations from Ref. [2–7].

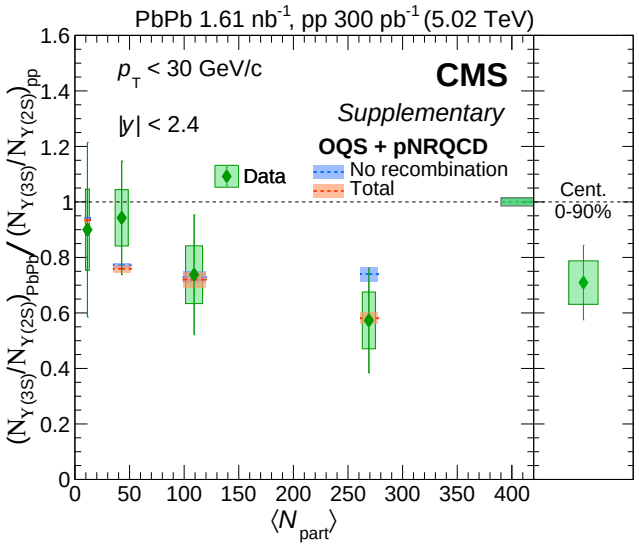

FIG. 17. The double ratio of $\Upsilon(3S)/\Upsilon(2S)$ as a function of $\langle N_{\mathrm{part}}\rangle$(from Figure 3 left). The vertical lines correspond to statistical uncertainties, while the boxes are the systematic uncertainties. The box at unity shows the combined systematic and statistical uncertainties from pp data. The orange and blue boxes represent calculations from Ref. [3], with the latter showing the calculations without the recombination component.

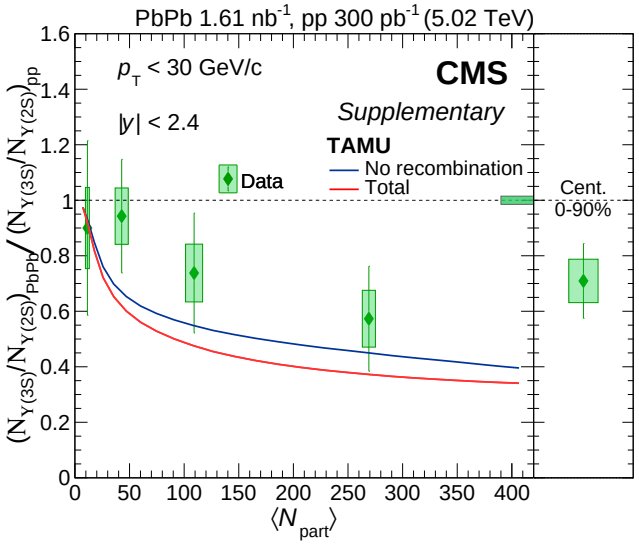

FIG. 18. The double ratio of $\Upsilon(3S)/\Upsilon(2S)$ as a function of $\langle N_{\mathrm{part}}\rangle$(from Figure 3 left). The vertical lines correspond to statistical uncertainties, while the boxes are the systematic uncertainties. The box at unity shows the combined systematic and statistical uncertainties from pp data. The red and blue lines represent calculations from Ref. [5], with the latter showing the calculations without the recombination component.

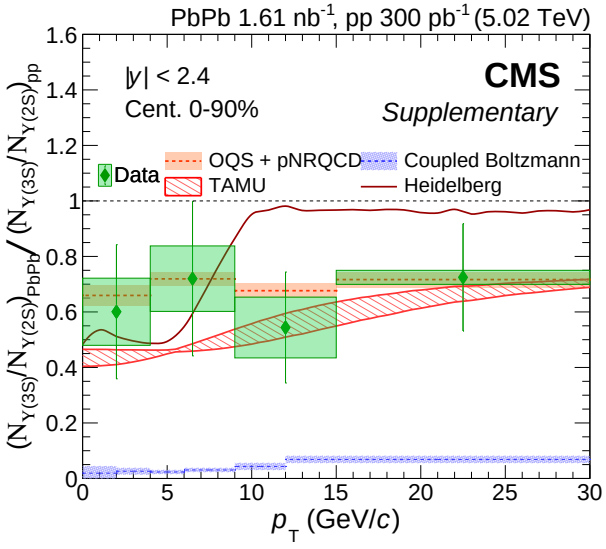

FIG. 19. The double ratio of $\Upsilon(3S)/\Upsilon(2S)$ as a function of p_T (from Figure 3 right). The vertical lines correspond to statistical uncertainties, while the boxes are the systematic uncertainties. The bands and line represent calculations from Ref. [2, 3, 5, 6].

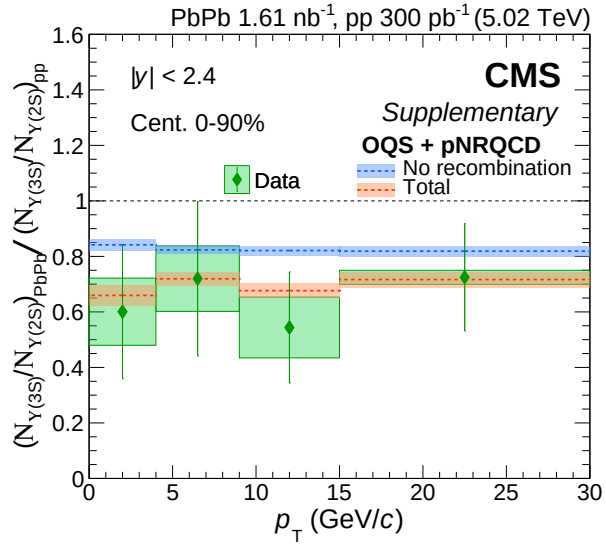

FIG. 20. The double ratio of $\Upsilon(3S)/\Upsilon(2S)$ as a function of p_T (from Figure 3 right). The vertical lines correspond to statistical uncertainties, while the boxes are the systematic uncertainties. The orange and blue bands represent calculations from Ref. [3], with the latter showing the calculations without the recombination component.

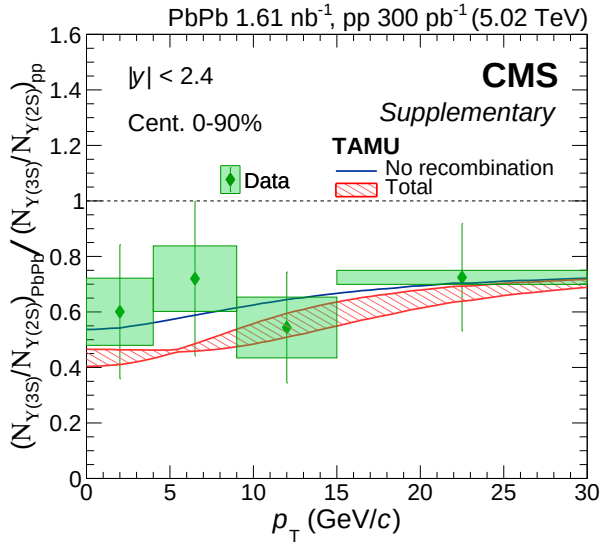

FIG. 21. The double ratio of $\Upsilon(3S)/\Upsilon(2S)$ as a function of p_T (from Figure 3 right). The vertical lines correspond to statistical uncertainties, while the boxes are the systematic uncertainties. The red band and blue line represent calculations from Ref. [5], with the latter showing the calculations without the recombination component.

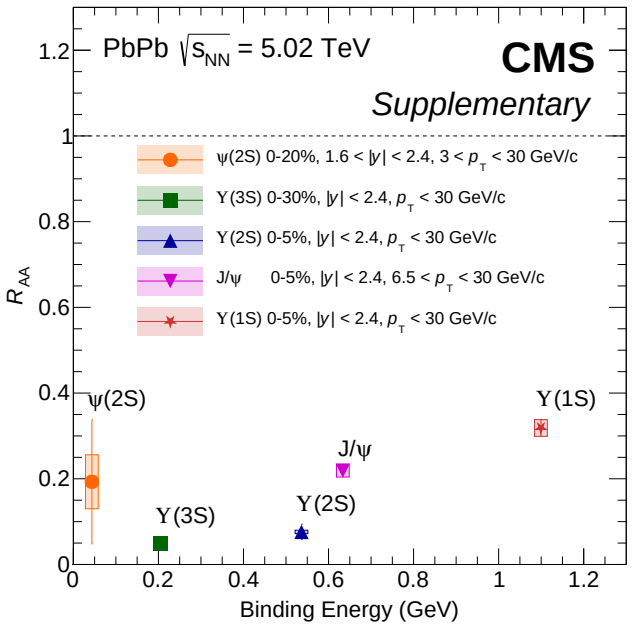

FIG. 22. The nuclear modification factors for various quarkonium mesons as a function of quarkonium binding energy at $\sqrt{s_{NN}} = 5.02$ TeV. The R_{AA} values are taken from the data point with the most central collision bin, e.g., the values for the Υ's correspond to the points of the hightest N_{part} in Figure 2 left. The values for the binding energy of each quarkonium state are taken from Ref. [8]. The error bars and boxes represent the statistical and systematic uncertainties, respectively. The results for the $\Upsilon(1S)$ meson and charmonium states (J/ψ and $\psi(2S)$) are taken from Refs. [1] and [9], respectively.

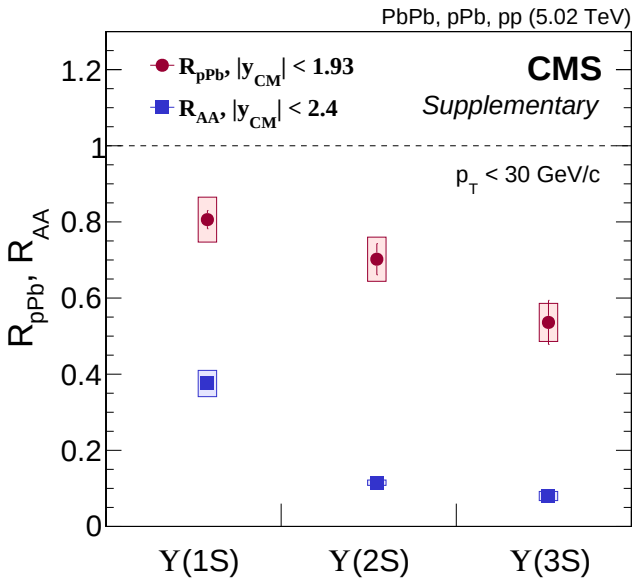

FIG. 23. The nuclear modification factors for $\Upsilon(1S)$, $\Upsilon(2S)$, and $\Upsilon(3S)$ mesons in pPb and PbPb collisions at $\sqrt{s_{NN}} = 5.02$ TeV. The error bars and boxes represent the statistical and systematic uncertainties, respectively. The $\Upsilon(2S)$ and $\Upsilon(3S)$ values are from the integrated bin in Figure 2 left. The results for pPb collisions and the $\Upsilon(1S)$ meson are taken from Refs. [10] and [1], respectively.

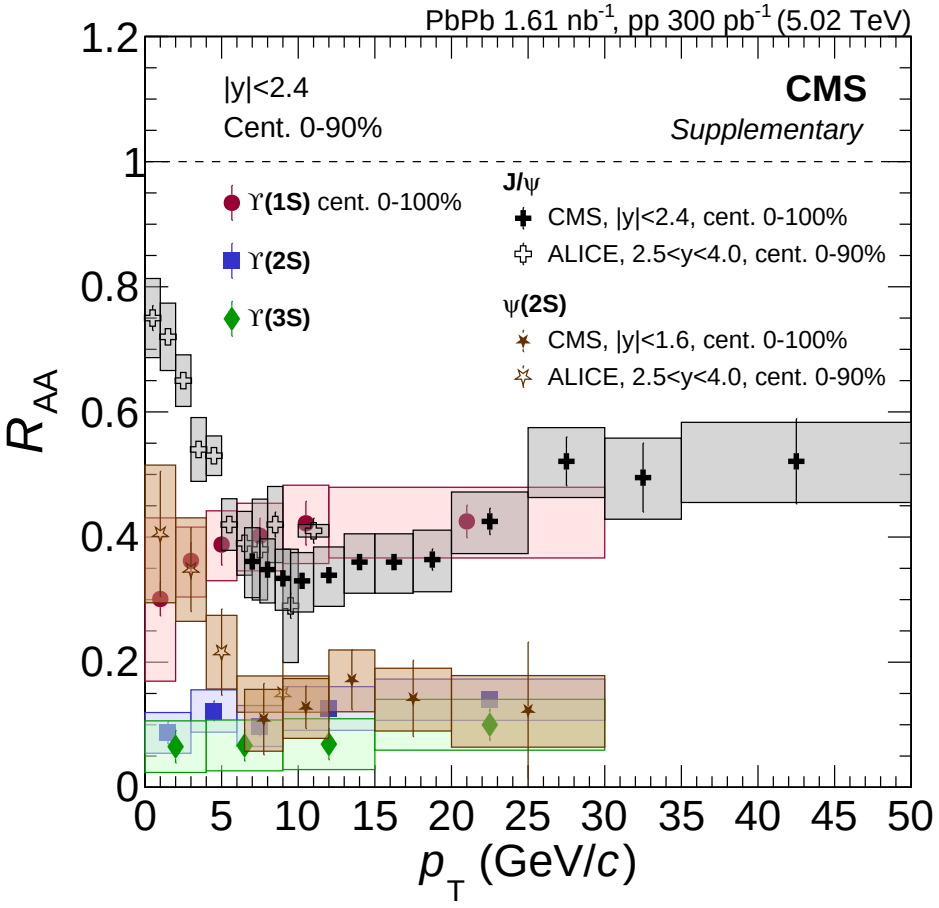

FIG. 24. Nuclear modification factors for the $\Upsilon(1S)$, $\Upsilon(2S)$, $\Upsilon(3S)$, J/ψ, and $\psi(2S)$ mesons as a function of p_{T}. The vertical lines and boxes correspond to statistical and systematic uncertainties, respectively. Results for the $\Upsilon(1S)$ meson are taken from Ref. [1]. The open and full cross points are the results for J/ψ mesons from Refs. [11] and [9], respectively. Results for $\psi(2S)$ mesons are taken from Refs. [12] and [9] for the open and full star points, respectively.

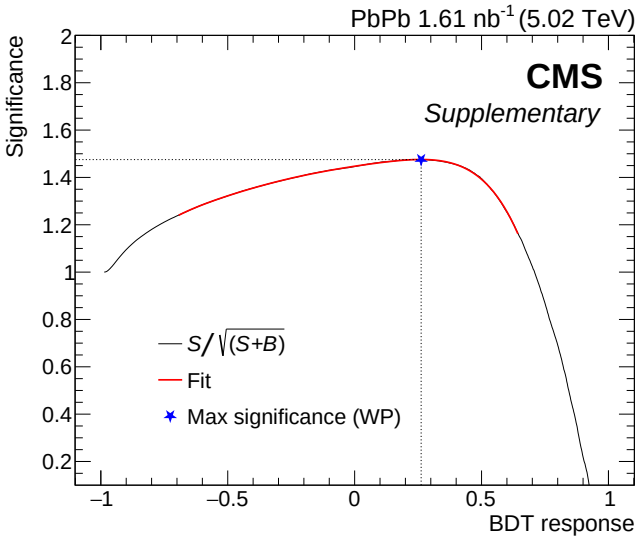

FIG. 25. The significance $S/\sqrt{S+B}$ for Υ mesons in PbPb collisions as a function of BDT score normalized to range between -1 and 1. The quantities S and B represent the yields of signal and background dimuons used for the BDT training, respectively. The working point (WP) is determined to be the BDT score that maximizes the significance using a parametic fit.

p_{T} range (GeV/c)	$\frac{1}{\langle T_{\mathrm{AA}}\rangle}\frac{d^2N^{\Upsilon}}{dp_{\mathrm{T}}dy}$	Stat. Unc.	Syst. Unc.
0–3	2.98	0.60	0.22
3–6	5.51	0.72	0.48
6–9	2.72	0.54	0.19
9–15	1.17	0.15	0.13
15–30	0.15	0.02	0.01

TABLE I. Yields for $\Upsilon(2S)$ mesons in PbPb collisions in centrality 0–90% and $|y| < 2.4$, corrected for acceptance and efficiency, and normalized by the nuclear thickness function $\langle T_{\mathrm{AA}}\rangle$ and the number of minimum bias events N_{MB}. The values for the yields and their uncertainties are in units of pb/ GeV/c.

Centrality	$\langle N_{\mathrm{part}}\rangle$	$\frac{1}{\langle T_{\mathrm{AA}}\rangle}\frac{d^2N^{\Upsilon}}{dp_{\mathrm{T}}dy}$	Stat. Unc.	Syst. Unc.
0–5%	382.30	1.02	0.25	0.08
5–10%	331.50	0.95	0.25	0.11
10–20%	262.30	1.31	0.20	0.14
20–30%	188.20	1.25	0.24	0.17
30–40%	131.00	1.71	0.29	0.13
40–50%	87.19	2.32	0.37	0.15
50–60%	54.42	3.27	0.51	0.32
60–70%	31.21	5.74	0.82	0.69
70–90%	11.43	7.80	1.26	1.10

TABLE II. Yields for $\Upsilon(2S)$ mesons in PbPb collisions in $p_{\mathrm{T}} < 30\,\mathrm{GeV}/c$ and $|y| < 2.4$, corrected for acceptance and efficiency, and normalized by the nuclear thickness function $\langle T_{\mathrm{AA}}\rangle$ and the number of minimum bias events N_{MB}. The values for the yields and their uncertainties are in units of pb/ GeV/c.

p_{T} range (GeV/c)	$\frac{1}{\langle T_{\mathrm{AA}}\rangle}\frac{d^2N^{\Upsilon}}{dp_{\mathrm{T}}dy}$	Stat. Unc.	Syst. Unc.
0–4	1.11	0.44	0.24
4–9	1.04	0.39	0.24
9–15	0.38	0.14	0.11
15–30	0.07	0.02	0.01

TABLE III. Yields for $\Upsilon(3S)$ mesons in PbPb collisions in centrality 0–90% and $|y| < 2.4$, corrected for acceptance and efficiency, and normalized by the nuclear thickness function $\langle T_{\mathrm{AA}}\rangle$ and the number of minimum bias events N_{MB}. The values for the yields and their uncertainties are in units of pb/ GeV/c.

[1] CMS Collaboration, Measurement of nuclear modification factors of $\Upsilon(1S)$, $\Upsilon(2S)$, and $\Upsilon(3S)$ mesons in PbPb collisions at $\sqrt{s_{\mathrm{NN}}} = 5.02\,\mathrm{TeV}$, Phys. Lett. B **790**, 270 (2019).

[2] X. Yao, W. Ke, Y. Xu, S. A. Bass, and B. Müller, Coupled Boltzmann transport equations of heavy quarks and quarkonia in quark-gluon plasma, J. High Energy Phys. **2021** (01), 046.

[3] N. Brambilla, M. . Escobedo, A. Islam, M. Strickland, A. Tiwari, A. Vairo, and P. V. Griend, Regeneration of bottomonia in an open quantum systems approach, Phys. Rev. D **108**, L011502 (2023).

[4] E. G. Ferreiro and J.-P. Lansberg, Is bottomonium suppression in proton-nucleus and nucleus-nucleus collisions at LHC energies due to the same effects?, J. High Energy Phys. **2018** (10), 094, [Erratum: doi: 10.1007/JHEP03(2019)063].

[5] X. Du, M. He, and R. Rapp, Color screening and regeneration of bottomonia in high-energy heavy-ion collisions, Phys. Rev. C **96**, 054901 (2017).

[6] G. Wolschin, Bottomonium spectroscopy in the quark gluon plasma, Int. J. Mod. Phys. A **35**, 2030016 (2020).

[7] A. Andronic, P. Braun-Munzinger, K. Redlich, and J. Stachel, Decoding the phase structure of QCD via particle production at high energy, Nature **561**, 321 (2018).

[8] H. Satz, Colour deconfinement and quarkonium binding, J. Phys. G: Nucl. Part. Phys. **32**, R25 (2006).

[9] CMS Collaboration, Measurement of prompt and nonprompt charmonium suppression in PbPb collisions at 5.02 TeV, The European Physical Journal C. **78**, 509 (2018).

[10] CMS Collaboration, Nuclear modification of Υ states in pPb collisions at $\sqrt{s_{\mathrm{NN}}} = 5.02\,\mathrm{TeV}$, Phys. Lett. B **835**, 137397 (2022).

[11] ALICE Collaboration, Studies of J/ψ production at forward rapidity in Pb-Pb collisions at $\sqrt{s_{\mathrm{NN}}} = 5.02$ TeV, J. High Energy Phys. **2020** (02), 041.

[12] ALICE Collaboration, $\psi(2S)$ suppression in Pb-Pb collisions at the LHC, arXiv:2210.08893 [nucl-ex] (2022).

Centrality	$\langle N_{\rm part}\rangle$	$\frac{1}{\langle T_{\rm AA}\rangle}\frac{d^2N^{\Upsilon}}{dp_{\rm T}dy}$	Stat. Unc.	Syst. Unc.
0–30%	269.10	0.33	0.10	0.07
30–50%	109.10	0.70	0.19	0.11
50–70%	42.81	1.85	0.36	0.21
70–90%	11.43	3.42	1.05	0.68

TABLE IV. Yields for $\Upsilon(3S)$ mesons in PbPb collisions in $p_{\rm T} < 30\,{\rm GeV}/c$ and $|y| < 2.4$, corrected for acceptance and efficiency, and normalized by the nuclear thickness function $\langle T_{\rm AA}\rangle$ and the number of minimum bias events $N_{\rm MB}$. The values for the yields and their uncertainties are in units of pb/ GeV/c.

Centrality	$\frac{1}{\langle T_{\rm AA}\rangle}\frac{d^2N^{\Upsilon}}{dp_{\rm T}dy}$	Stat. Unc.	Syst. Unc.
0–5%	15.20	0.89	$^{+0.88}_{-0.95}$
5–10%	15.28	1.01	$^{+0.89}_{-0.96}$
10–20%	15.40	0.82	$^{+0.94}_{-1.00}$
20–30%	19.12	1.86	$^{+1.22}_{-1.27}$
30–40%	23.06	1.29	$^{+1.68}_{-1.71}$
40–50%	24.95	1.70	$^{+2.18}_{-2.14}$
50–60%	28.96	2.51	$^{+3.10}_{-3.00}$
60–70%	43.89	4.17	$^{+6.04}_{-5.56}$
70–100%	37.69	6.21	$^{+6.68}_{-4.61}$

TABLE V. Yields for $\Upsilon(1S)$ mesons in PbPb collisions in $p_{\rm T} < 30\,{\rm GeV}/c$ and $|y| < 2.4$, corrected for acceptance and efficiency, and normalized by the nuclear thickness function $\langle T_{\rm AA}\rangle$ and the number of minimum bias events $N_{\rm MB}$ from Ref. [1]. The values for the yields and their uncertainties are in units of pb/ GeV/c.